



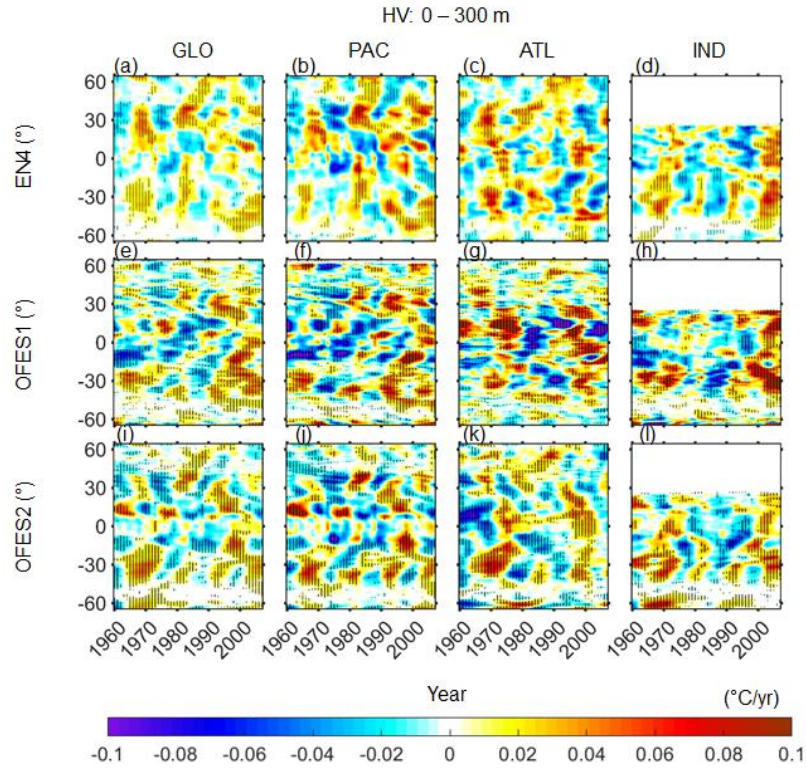
Supplement of

Comparison of ocean heat content estimated using two eddy-resolving hindcast simulations based on OFES1 and OFES2

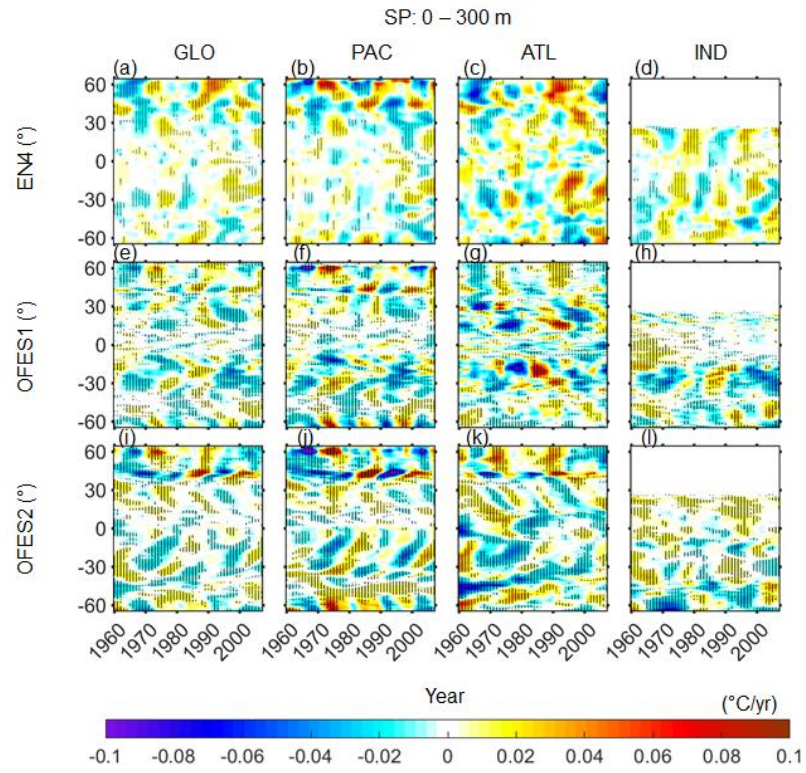
Fanglou Liao et al.

Correspondence to: Zhiqiang Liu (liuzq@sustech.edu.cn) and Xiao Hua Wang (x.h.wang@unsw.edu.au)

The copyright of individual parts of the supplement might differ from the article licence.

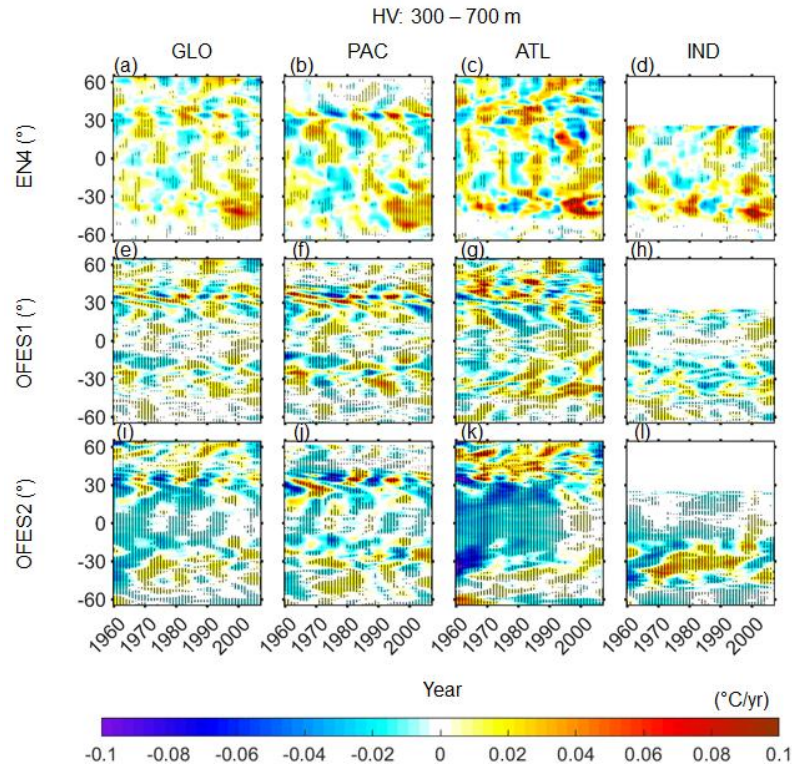


31
 32 **Figure S1.** Temporal evolution of the 10-year rolling trend of the HV component of the zonal-averaged potential temperature
 33 change for the top ocean layer (0–300 m). **Left to right:** global, Pacific, Atlantic and Indian Oceans. **Top to bottom:** EN4,
 34 OFES1 and OFES2. Horizontal axis: year; vertical axis: latitude. Stippling indicates the 95% confidence level.
 35
 36
 37



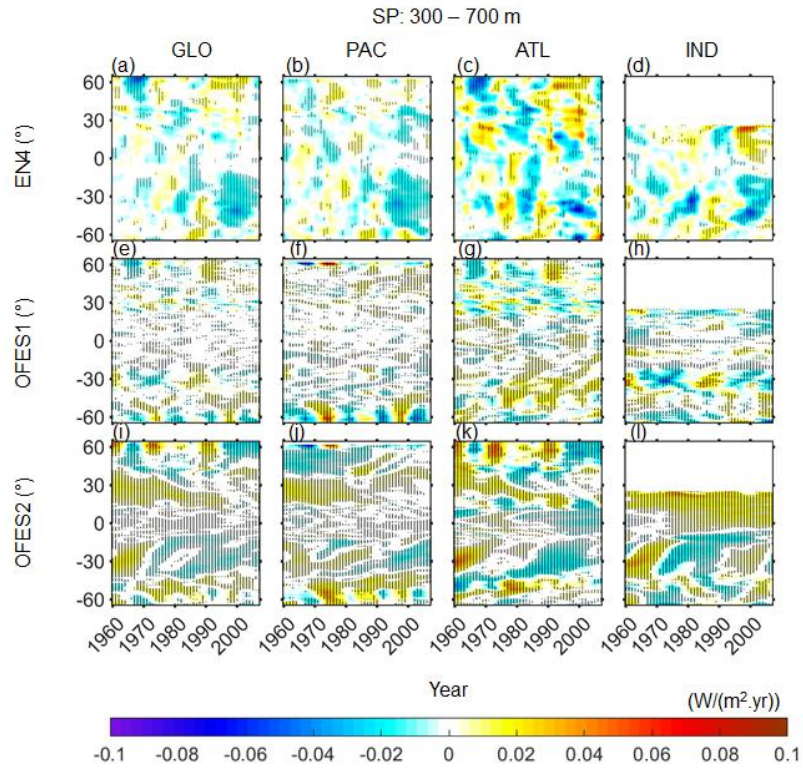
38
39
40
41
42
43
44

Figure S2. As for Fig. S1 but for the SP component.



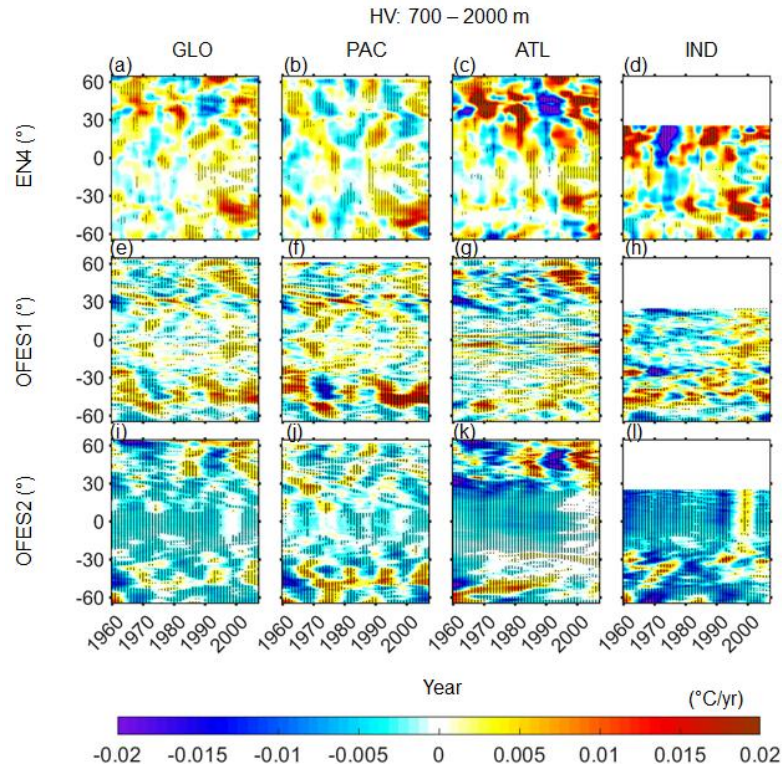
45
46
47
48
49
50
51

Figure S3. Temporal evolution of the 10-year rolling trend of the HV component of the zonal-averaged potential temperature change for the middle ocean layer (300–700 m). **Left to right:** global, Pacific, Atlantic and Indian Oceans. **Top to bottom:** EN4, OFES1 and OFES2. Horizontal axis: year; vertical axis: latitude. Stippling indicates the 95% confidence level.



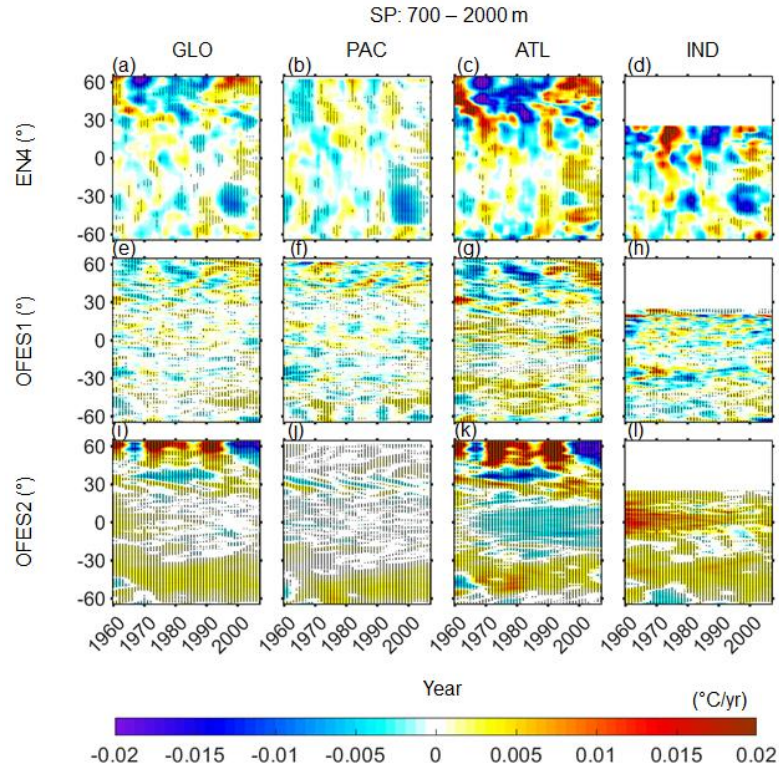
52
53
54
55
56
57

Figure S4. As for Fig. S3 but for the SP component.



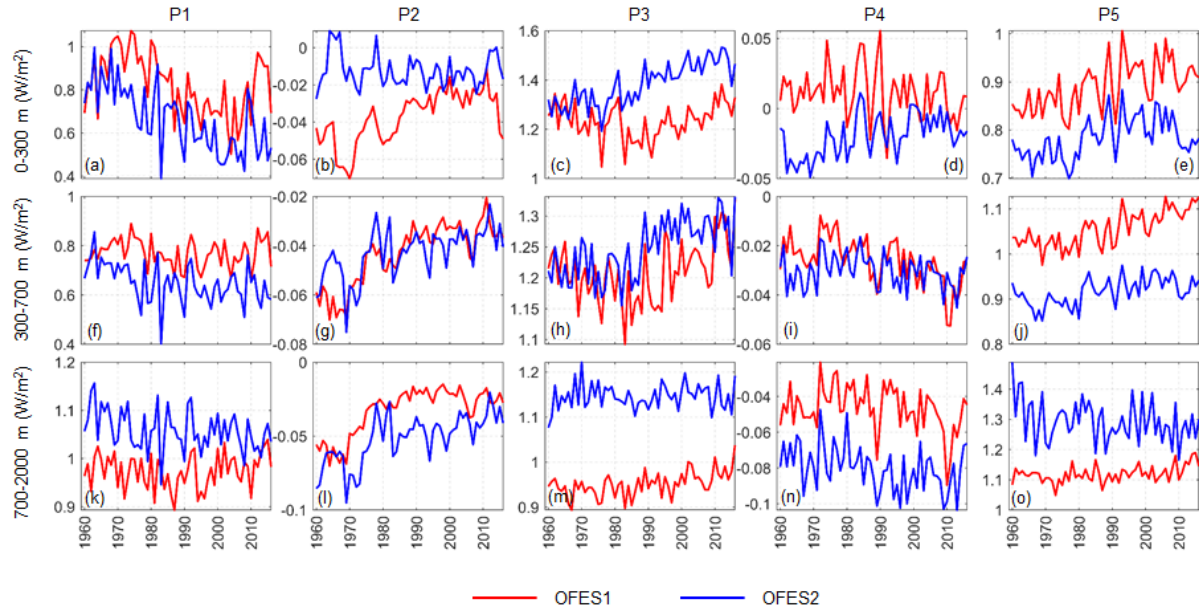
58
59
60
61
62
63

Figure S5. Temporal evolution of the 10-year rolling trend of the HV component of the zonal-averaged potential temperature change for the bottom ocean layer (700–2000 m). **Left to right:** global, Pacific, Atlantic and Indian Oceans. **Top to bottom:** EN4, OFES1 and OFES2. Horizontal axis: year; vertical axis: latitude. Stippling indicates the 95% confidence level.



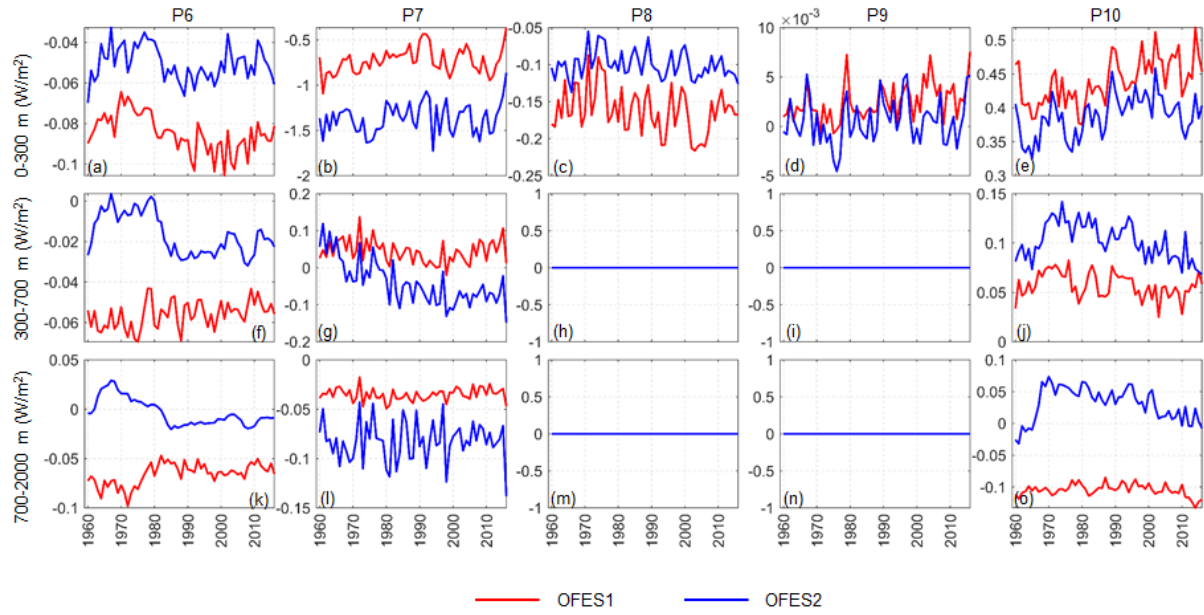
64
65
66
67
68
69
70
71
72
73
74

Figure S6. As for Fig. S5 but for the SP component.



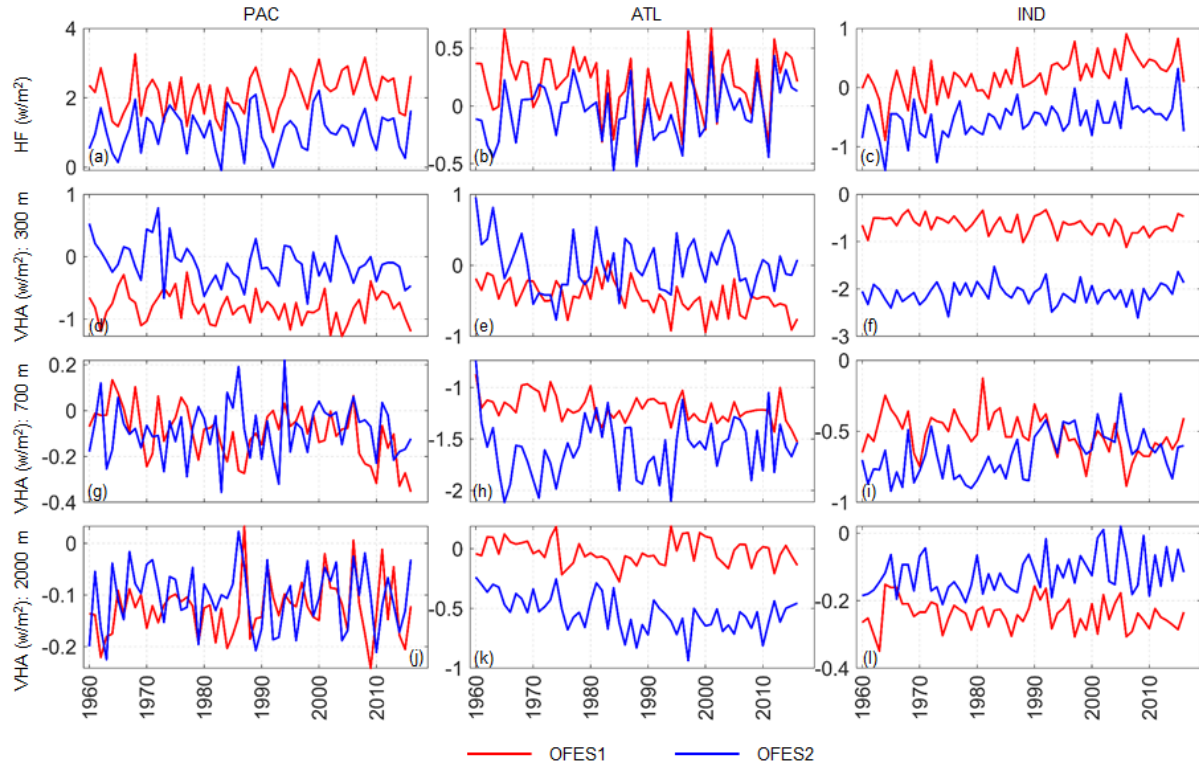
75
 76
 77
 78
 79
 80
 81
 82
 83
 84
 85
 86
 87

Figure S7. Time series of heat advection through the P1–P5 from left to right. **Top to down:** 0–300 m, 300–700 m and 700–2000 m. The red line is for the OFES1 and blue for the OFES2. The heat advection was converted to an equivalent heat flux applied over the entire surface of the Earth. Note different vertical axis scale was used for a better visualization.



88
 89
 90
 91
 92
 93
 94
 95
 96

Figure S8. As for Fig. S7 but for the P6–P10. Note that there was no heat advection through the P8 and P9 below 300 m.



97

98 **Figure S9.** Time series of net basin-integrated surface heat flux (HF) and vertical heat advection (VHA). **Left to right:** the Pacific,
 99 Atlantic and Indian Oceans. **Top to down:** HF, VHA at 300 m, VHA at 700 m and VHA at 2000 m. The red line is for the OFES1
 100 and blue for the OFES2. Note different vertical axis scale was used for a better visualization.

101

102

103

104

105

106

107

108

109

110

111

112

113

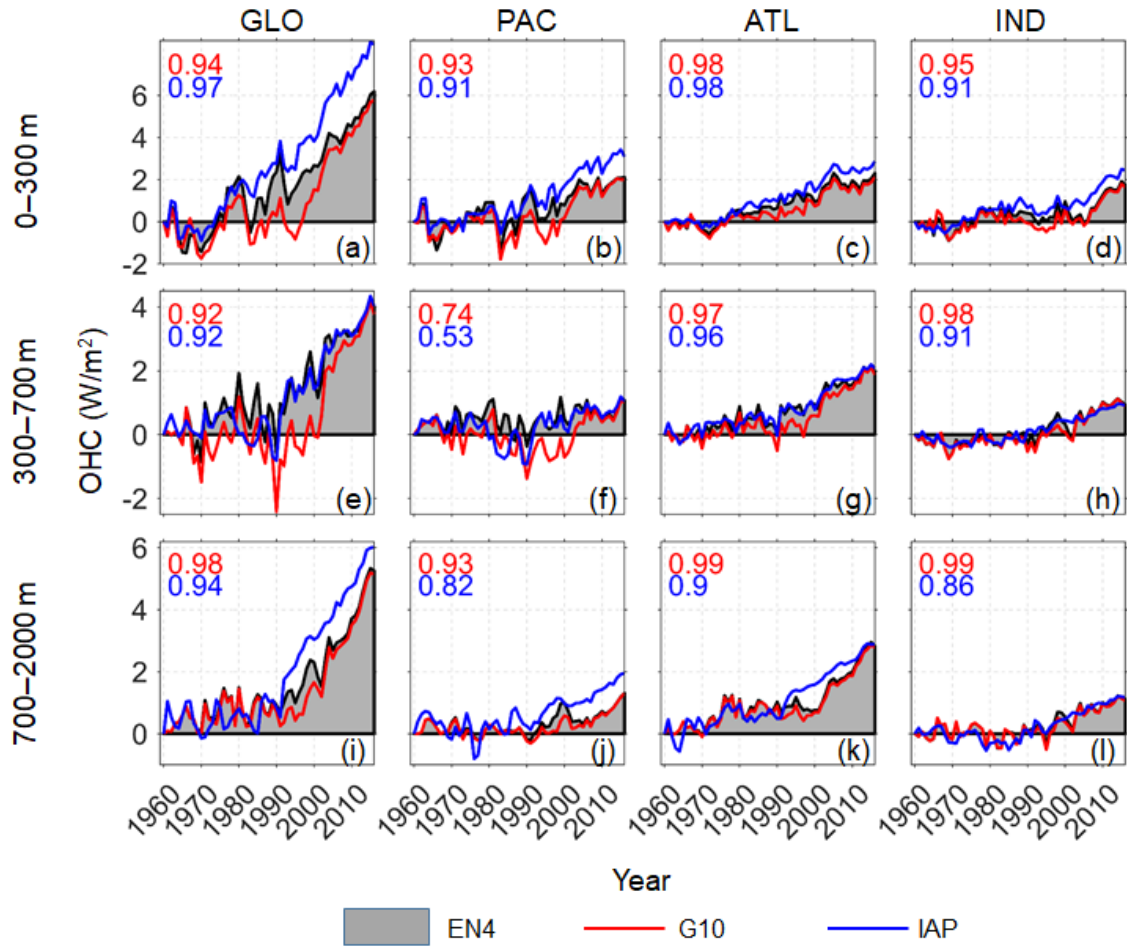
114

115

116

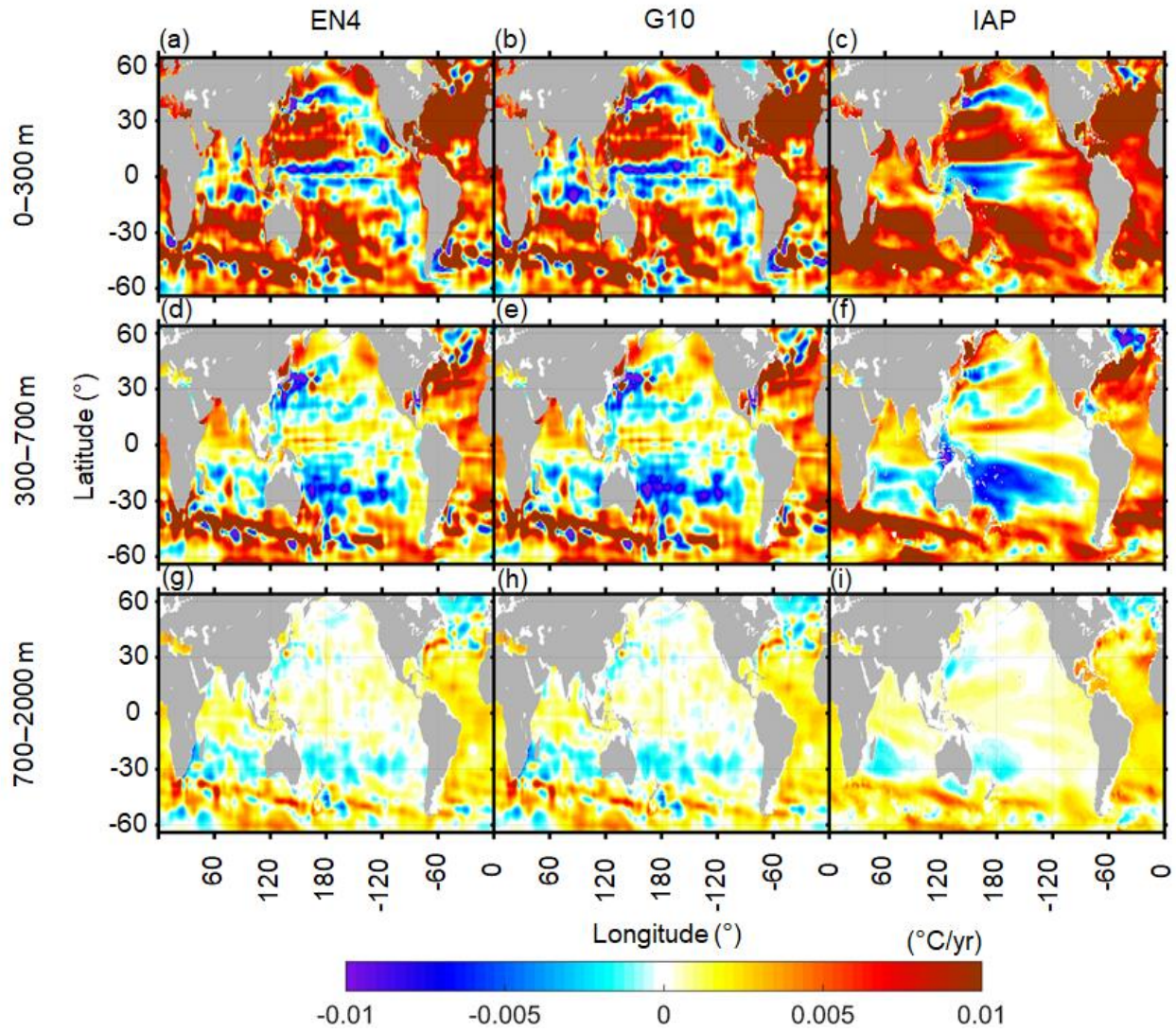
117

118



119
 120
 121
 122
 123
 124
 125
 126
 127
 128
 129
 130
 131
 132
 133
 134
 135
 136
 137

Figure S10. As for Fig. 2 but is a comparison between the OHC from EN4, G10 and IAP. **Left to right:** the global ocean, Pacific Ocean, Atlantic Ocean and Indian Ocean. **Top to down:** the upper layer (0–300 m), middle layer (300–700 m) and lower layer (700–2000 m). Numbers on the left top corners are the correlation coefficients between the G10 (red) or IAP (blue) and EN4. Note that EN4 here is the EN4.2.1 with bias corrected following Levitus et al. (2009); G10 is the most up to date version of EN4 datasets (EN4.2.2) with bias corrected following Gouretski and Reseghetti (2010); and IAP is the dataset from the Institute of Atmospheric Physics (Cheng and Zhu, 2016).



138

139 **Figure S11.** As for Fig. 14 but is a comparison between the OHC from EN4, G10 and IAP. **Left to right:** the EN4, G10 and IAP.

140 **Top to down:** the upper layer (0–300 m), middle layer (300–700 m) and lower layer (700–2000 m).